Cone-beam computed tomography artifacts in the presence of dental implants and associated factors: An integrative review

Bianca Rodrigues Terrabuio[ID][1], Caroline Gomes Carvalho[ID][1], Mariela Peralta-Mamani[ID][1],
Paulo Sérgio da Silva Santos[ID][1], Izabel Regina Fischer Rubira-Bullen[ID][1,*], Cássia Maria Fischer Rubira[ID][1]

[1]*Department of Surgery, Stomatology, Pathology, and Radiology, Bauru School of Dentistry, University of São Paulo, SP, Brazil*

ABSTRACT

Purpose: This study was conducted to review the literature regarding the types of cone-beam computed tomography (CBCT) artifacts around dental implants and the factors that influence their formation.

Materials and Methods: A search strategy was carried out in the PubMed, Embase, and Scopus databases to identify published between 2010 and 2020, and 9 studies were selected. The implants included 306 titanium, titanium-zirconium, and zirconia implants, as well as 5 titanium cylinders.

Results: The artifacts around the implants were the beam-hardening artifact, the streaking artifact, and band-like radiolucent areas. Some factors that influenced the formation of artifacts were the implant material, bone type, evaluated regions, distance, type of CBCT, field of view (FOV) size, milliamperage, peak kilovoltage (kVp), and voxel size. The beam-hardening artifact was the most widely reported, and it was minimized in protocols with a smaller FOV, larger voxels, and higher kVp.

Conclusion: The risk and benefit of these protocols in individuals with dental implants must be considered, and clinical examinations and complementary radiographs play an essential role in implantology. *(Imaging Sci Dent 2021; 51: 93-106)*

KEY WORDS: Artifacts; Cone-Beam Computed Tomography; Dental Implants; Review

Introduction

In dentistry, cone-beam computed tomography (CBCT) provides 3-dimensional images with advantages over conventional tomography, such as lower radiation doses and easier image acquisition.[1-3] The tomography is based on the emission of a cone-shaped X-ray beam in a 360° rotation, through which the entire volume of structures is obtained. The images are reconstructed through a computer system volumetrically, bi-dimensionally, and three-dimensionally.[4]

Thanks to its advantages, CBCT has become essential in dentistry and its various specialties. In implantology, linear measurements, of both depth and height, improve safety and provide new possibilities in oral rehabilitation that require osseointegrated implants, since CBCT enables the accurate localization of anatomical structures and quantification of the remaining bone.[5]

Although there are numerous advantages to CBCT images, limitations are encountered. The most frequently encountered problem is the formation of image artifacts.[6] This problem occurs due to several factors, including low milliamperage (mA) and peak kilovoltage (kVp) used in image acquisition, which cause a higher amount of radiation to be dissipated in the presence of high-density elements, resulting in significant changes that compromise the image and, consequently, the diagnosis.[2,7]

An image artifact can be defined as a structure that is visualized next to the image formed through the data used in the reconstruction, but is not present in the object in which the shot was taken. The artifact is caused by discrepancies between the mathematical format used to perform the 3-dimensional reconstruction and the actual physical condi-
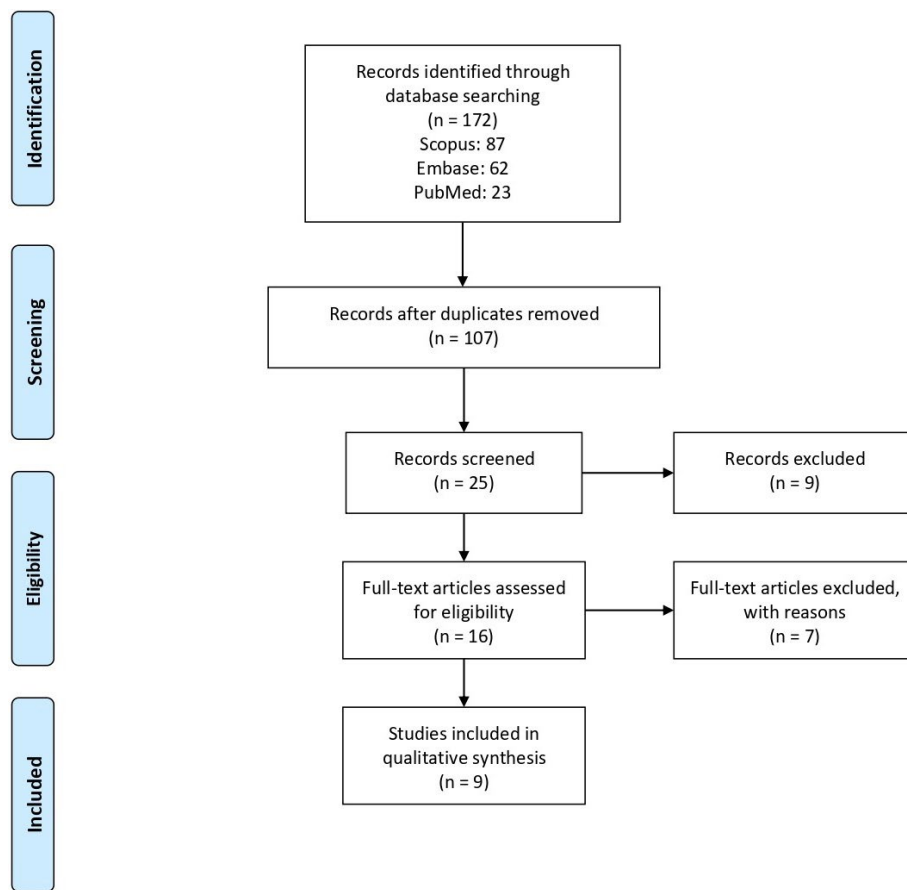
Fig. 1. Flow diagram.

tions.[8,9]

Artifacts have different origins; they can be caused by factors related to the acquisition of images or by physical factors of the device. When caused by the patient, they are related to the presence of metallic materials in the examination area and the patient's movement during image acquisition. Reconstruction artifacts, in contrast, result from errors in the reconstruction of the acquired sections.[5,10]

To facilitate understanding, artifacts can be divided according to the factors responsible for their origin. The main artifacts include motion artifacts, ring artifacts, artifacts generated by very dense materials, scattering artifacts, noise artifacts, extinction artifacts, and cone-beam effect artifacts.[5] Therefore, the objective of this work was to present an integrative literature review on the types of artifacts and the factors that influence their formation around osseointegrated dental implants in CBCT.

Materials and Methods

This integrative review was carried out by collecting data from carefully selected articles, for which it was possible to scrutinize the results obtained. The research question was: What types of artifacts are present in CBCT exams with dental implants and what are the factors that influence their formation? All studies met the criteria established by the PECO strategy: the participants (P) were patients and phantoms with dental implants; the exposure (E) was CBCT exams; no control (C) was considered; and the outcomes (O) were types of artifacts and factors that influence their formation.

To identify the studies to be included, a search strategy was developed based on the descriptors "cone-beam computed tomography," "dental implants," and "artifacts," and applied to the electronic databases PubMed, Embase, and Scopus. The articles were imported into the reference manager EndNote Web for organizing and excluding duplicates from different databases (Fig. 1).

The inclusion criteria were articles in English that were published in the last 10 years, encompassing all types of clinical studies (retrospective, prospective, cross-sectional, etc.) or *in vitro* studies only with a CBCT sample, that re-

ported research on the theme of different types of artifacts present in CBCT exams with dental implants. The exclusion criteria were case reports, review articles, letters to the editor, and articles that reported the basic principles of CBCT, artifacts around implants in multislice computed tomography (MSCT), bone evaluation for dental implants, mandibular positioning through CBCT, artifacts unrelated to dental implants, artifact reduction, the application of CBCT in implantology, the radiation dose of CBCT compared to MSCT, and comparisons of artifacts in implants before and after metal artifact reduction.

The final selection of the studies and data extraction were carried out by 2 researchers (B.R.T. and C.G.C.), and disagreements between them were resolved by a third researcher (M.P.M.). The qualitative and quantitative data extracted from the selected studies were organized in a table in chronological order and described. A narrative synthesis of the data was performed (Table 1).

Results

With the search strategies used in the databases, a total of 183 studies were identified, of which only 172 were published in the last 10 years. The further exclusion of 65 duplicate articles resulted in 107 articles. Based on the title and abstract, 25 articles were pre-selected. Nine studies were excluded for not meeting the eligibility criteria. Sixteen studies were selected for full-text reading, after which 7 studies were excluded because they dealt with topics related to artifact reduction, the evaluation of peri-implant tissue, and comparisons between the implant radiation dose of CBCT and MSCT,[11-17] yielding a final total of 9 selected articles.[18-26]

Types of studies, sample size, and characteristics

The articles included in this review presented *in vitro* studies (n = 7)[18-21,23,25,26] and clinical studies with tomography of patients (n = 2).[22,24] They were carried out in Brazil (n = 3), Switzerland (n = 2), Germany (n = 1), Japan (n = 1), Iran (n = 1), and USA/Turkey (n = 1). The *in vitro* studies used phantoms of different materials, such as plaster type IV and polymethylmethacrylate, dry human jaws, and bone blocks. Only 1 of the CBCT studies of patients specified the number of patients (n = 22), age (23-74 years), and sex (7 men and 15 women). The other clinical study included patients of varying ages and both sexes.

The implants were made of titanium (n = 291), titanium grade 4 (n = 1), titanium grade 5 (n = 1), titanium-zirconia (n = 6), and zirconia/zirconia dioxide (n = 7), totaling 306

Table 1. Data extracted from included studies

Author (year)	Country	Study	Population	Tomograph	Protocol	CBCT image evaluation	Implant and region	Artefact's type	Voxel, FOV, implant material and tomograph influence	Prevalence according to implant location and distance of artifacts in the anatomical region
Martins et al. (2020)[18]	Brazil	*In vitro*	- Three cylindrical polymethyl methacrylate plate phantoms - Five bone cylinders with trabecular and cortical bones from a fresh bovine rib Measurements were made around this tissue.	- OP300 MAXIO® - Picasso Trio®	- 90 kVp - 3.2 mA - Voxel: 0.2 mm - FOV (OP300 MAXIO): 8 × 15 cm - FOV (Picasso Trio): 8.5 × 12 cm - With and without activation of the MAR protocol	- ImageJ (NIH, Bethesda, MD) - Reconstruction: The trabecular level was used sagittally to measure the distances from the endosteal surface plate until the middle point of the cylinder (3.25 mm). For cortical bone level was used axial, 4.25 mm under the middle point. - ROI: 8 regions around the bone (buccal, mesio-buccal, mesial, mesio-lingual, lingual, disto-lingual, distal, and disto-buccal)	- Titanium cylinders (14.5 mm × 5.5 mm) (S.I.N. Implantes, São Paulo, Brazil) - Implant regions protocol: 1) Control: AR, no metal 2) A: 1 posterior on the opposite side of the AR 3) B: 2 posterior on the opposite side of the AR 4) C: 2 posterior and 1 anterior on the opposite side of the AR 5) D: 1 posterior on the adjacent side of the AR 6) E: 2 posterior on the adjacent side of the AR 7) F: 2 posterior and 1 anterior on the adjacent side of the AR	Beam-hardening	- Picasso Trio expressed more artifacts than OP300 MAXIO, regardless of the protocol	- The expression of artifacts was greater in the cortical bone, in both tomographs. - In the presence of 3 implants adjacent to the bone cylinder (2 distal and 1 mesial), there were more artifacts than in other protocols.

Table 1. Continued

Author (year)	Country	Study	Population	Tomograph	Protocol	CBCT image evaluation	Implant and region	Artefact's type	Voxel, FOV, implant material and tomograph influence	Prevalence according to implant location and distance of artifacts in the anatomical region
Demirturk Kocasara et al. (2019)[19]	USA and Turkey	*In vitro*	- Three phantoms with zirconium, titanium and titanium-zirconium implants embedded in the ultrasound gel	- i-CAT 3-D Imaging System®	- 120 kVp - 20.27 mAs - FOV: 16 × 13 cm - Voxel: 0.2 mm, 0.25 mm, 0.3 mm, 0.4 mm - Scan time: 14.7 s (voxel: 0.2 mm and 0.25 mm) and 4.8 s (voxel: 0.3 mm and 0.4 mm)	- Image J (NIH, Bethesda, MD) - Reconstruction: Axial	- Zirconium implant - Titanium grade 4 implant - Titanium grade 5 implant - Titanium-zirconium implant	Streaking and beam-hardening	- The zirconium implant presented more artifacts, followed by the titanium grade 4 implant, titanium-zirconium implant and titanium grade 5 implants. - The 0.2-mm voxels showed more artifacts, followed by the 0.25-mm voxels. - The 0.3-mm and 0.4-mm voxels were similar.	–
Shokri et al. (2019)[20]	Iran	Experimental - *in vitro*	- Fresh bovine bone with 4 blocks: D1: completely cortical bone D2 and D3: cortical and cancellous bone D4: cancellous bone - Height and mesiodistal width of 10 mm and thickness of 6.5 mm - Soft tissue simulation: red wax - Mandibular wax model was used in the large FOV	- Cranex 3D® (Soredex, Tuusula, Finland).	CBCT protocols: - FOV: 4 × 6 cm², 4 T: 6.1 s kVp: 90, Rotation time: 10 s; voxel 0.136 mm - FOV: 4 × 6 cm², 10 T: 6.1 s kVp: 90, Rotation time: 10 s; voxel 0.136 mm - FOV: 6 × 8 cm², 4 T: 12.6 s kVp: 90, Rotation time: 20 s; voxel 0.2 mm - FOV: 6 × 8 cm², 10 T: 12.6 s kVp: 90, Rotation time: 20 s; voxel 0.2 mm	- OnDemand 3D Dental software (Cybermed, Seoul, Korea) - Reconstruction: Cross-section sections displaced, the middle area of each bone was used to determine the mean GV. - ROI: buccal surface, 3 to 7 mm apically to the implant shoulder - GV: subtracting before and after implant placement for artifact calculation	- Nine implants: DIO (Centum seo-ro, Haeundae-gu, Busan, Korea), PSI type with a 3.5-mm diameter and 10-mm length - Implant region: randomly placed in each mold	Beam-hardening	- The mean GV: - Large FOV, 4 mA shows more artifacts, followed by large FOV, 10 mA, small FOV, 4 mA and small FOV, 10 mA showed less artifacts. - Cancellous bone had more artifacts, followed by cortical and cancellous bone, and less artifacts were found in cortical bone. - Cancellous bone had significantly higher amount of artifacts than other groups ($P < 0.05$). - Increasing the mA did not decrease the metal artifacts.	–

Table 1. Continued

Author (year)	Country	Study	Population	Tomograph	Protocol	CBCT image evaluation	Implant and region	Artefact's type	Voxel, FOV, implant material and tomograph influence	Prevalence according to implant location and distance of artifacts in the anatomical region
Fontenele et al. (2018)[21]	Brazil	*In vitro*	- Two dry human mandibles - Soft tissue simulation was used in a cylindrical water container (16 cm diameter).	- Picasso Trio 3D® - ProMax 3D® - 3D Accuitomo 80®	- 80 kVp - 5 mA - FOV (Picasso Trio and ProMax): 8×5 cm - FOV (Accuitomo): 8×8 cm - Voxel: 0.2 mm - Scan time: 24 s (Picasso Trio), 17.5 s (Accuitomo) and 12 s (ProMax) - Frames: 720 (Picasso Trio), 640 (Accuitomo) and 251 (ProMax)	- Image J (NIH, Bethesda, MD) - Reconstruction: axial - ROI: 11 regions No region was adjacent to the implant, but the region corresponding to the buccal floor was superimposed.	- Titanium implants 4×11 mm (Titamax, Neodent, Brazil) - Zirconium oxide implants 4×11 mm (Z-Look3, Z-systems, Switzerland) - Implant region: edentulous region of tooth 46	Beam-hardening	- Zirconium oxide implants had a greater amount of artifacts than titanium implants. - Tomographs: for titanium implants, Accuitomo presented more artifacts than ProMax and Picasso Trio, which had similar results. - For zirconium implants, Accuitomo presented more artifacts, followed by ProMax and Picasso Trio.	- The greater the distance from the evaluated area of the implant, the smaller the amount of artifacts. - The artifacts reached up to 3.5 cm from the object generating the artifact.
Machado et al. (2018)[22]	Brazil	Retrospective	- 200 implants were divided according to their location: anterior maxilla, posterior maxilla, anterior mandible, and posterior mandible. - The selection of the sample was defined at random, until each group had 50 implants.	- i-Cat Next Generation®	- 120 kV - 8 mA - 26.9 s rotation - Voxel: 0.25 mm - FOV between 6×16 and 8×16 cm	- Radiant DICOM software (Medixant, Poznan, Poland) - Reconstruction: 3 axial for each implant - ROI: in the apical, middle and cervical third. Circular ROI, 10 mm diameter - Artifact analysis: ImageJ software (US National Institutes of Health, Bethesda, MD). - GV: According to Pauwels et al. (2013) methods.	- Titanium implants, external hexagon with lengths of 4 to 13 mm and diameters of 3.5 to 4 mm	Beam-hardening	–	- The mandible showed higher artifacts in the apical (17.69) and middle (18.48) images than in the maxilla (P<0.05). - The anterior region implants showed higher artifacts in the apical (17.48) and middle (17.93) images than in the posterior region (P<0.05). - Adjacent implants showed higher artifacts than isolated implants in the apical and middle third. - Comparing the images, higher artifacts were always observed in the cervical third.

Table 1. Continued

Author (year)	Country	Study	Population	Tomograph	Protocol	CBCT image evaluation	Implant and region	Artefact's type	Voxel, FOV, implant material and tomograph influence	Prevalence according to implant location and distance of artifacts in the anatomical region
Sancho-Puchades, Hämmerle, Benic. (2014)[23]	Switzerland	Experimental - in vitro	- Twenty test mandible models (using type IV dental stone)	- i-CAT Next-Generation scanner®	- 120 kV acceleration voltage - 5 mA beam current - FOV: diameter of 16 cm, FOV height of 6 cm, 600 projections, 360° rotation - Voxel: 0.25 mm - Scan time: 26 s	- eXam Vision imaging software (KaVo Dental GmbH) - Reconstruction: axial - ROI: 8 regions (0.25 mm × 0.25 mm) in the axial plane and 4 mm in the implant long axis. Along the implant axis, ROIs were set from 3 to 7 mm apically to the implant shoulder. - X-ray attenuation: GV, conversion to UCLA (color-lookup-table), using OsiriX 3.7 imaging software (OsiriX Foundation, Geneva, Switzerland)	Titanium implants: Straumann® Standard Plus, Regular Neck; Institut Straumann AG, Basel, Switzerland - Cylindrical 4.1 mm × 4.8 mm diameter × 10 mm length (Ti4.1) - Cylindrical 3.3 mm × 4.8 mm diameter × 10 mm length (Ti3.3) - Titanium-zirconium: cylindrical 3.3 mm × 4.8 mm diameter × 10 mm length (TiZr3.3) - Zirconium dioxide monotype implants: conical 3.5-4.5 mm × 4.5 mm diameter × 10 mm length (ZrO3.5-4.5) (VITA Zahnfabrik, Bad Säckingen, Germany) - Implant region: the single-tooth gap 45	Beam-hardening	- The ZrO3.5-4.5 showed highest artifacts (range: −156% to 269%), followed by TiZr3.3 (range: −55% to 87%), Ti4.1 (range: −46% to 98%) and Ti3.3 implants (range: −11% to 84%) ($P \leq 0.0167$).	- More artifacts were shown buccally, mesio-buccally, lingually, and disto-lingually than mesially and distally. - The GV reduced with the increasing distance from the implant surface.
Naitoh et al. (2013)[24]	Japan	Prospective	- Twenty-one patients (7 men and 15 women) with a mean age of 56.3 years (23-74 years). - A total of 61 implants were assessed.	- Alphard VEGA® (Asahi Roentgen Ind., Co., Kyoto, Japan)	- 80 kV - 5 mA - FOV: 102 mm in diameter and 60 or 102 mm in height - Voxel size: 0.2 × 0.2 × 0.2 mm	- OsiriX Imaging Software; The OsiriX Foundation, Geneva, Switzerland - Reconstruction: a longitudinal 2D image - ROI: between dental implants (n = 33), between dental implants and neighboring teeth (n = 36), posterior to dental implants (n = 21), and between neighboring teeth (n = 29) - Artifact evaluation: the mean pixel value in ROIs	Titanium implants: - Replace Tapered implant system, n = 57 - Brånemark implant system, n = 4 Both: Nobelbiocare, Goteborg, Sweden The length was 10 mm (n = 38) and 13 mm (n = 23). The diameter of implants was a regular platform (n = 55), a narrow platform (n = 1), and a wide platform (n = 5). - Implant region: mandibular posterior. Mean follow-up: 25.0 months (SD, 14.7 months)	Band-like radiolucent areas	–	- There was more artifacts between dental implants (−97, SD 285), followed by posterior to dental implants (163, SD 234), between dental implants and neighboring teeth (411, SD 241) and between neighboring teeth (600, SD 231).

Table 1. Continued

Author (year)	Country	Study	Population	Tomograph	Protocol	CBCT image evaluation	Implant and region	Artefact's type	Voxel, FOV, implant material and tomograph influence	Prevalence according to implant location and distance of artifacts in the anatomical region
Benic et al. (2012)[25]	Switzerland	In vitro	- Ten test mandible models - Material: type IV dental stone (Noritake Super Rock; Noritake Co., Nagoya, Japan) - Control: 3 test mandible models without implants	- 3D eXam CBCT®	- 120 kV - 5 mA - FOV diameter: 16 cm - FOV height: 6 cm - Projections: 600 - Rotation: 360° - Voxel: 0.25 mm - Scan time: 26 s	- eXam Vision imaging software (KaVo Dental GmbH, Biberach, Germany) - Reconstruction: axial - ROI: 8 regions (0.25 mm × 0.25 mm) in the axial plane and 4 mm in the implant long axis. Along the implant axis, ROIs were set from 3 to 7 mm apically to the implant shoulder. - X-ray attenuation: GV, conversion to UCLA (color-lookup-table), using OsiriX 3.7 imaging software (OsiriX Foundation, Geneva, Switzerland)	- Titanium implants: 4.1 mm × 10 mm (Straumann® Dental Implant System; Straumann AG, Basel, Switzerland) - Implant region: edentulous regions of teeth 37, 36, 34, 33, 31, 41, 43, 44, 46 and 47	Beam-hardening	–	- Artifacts were always present in the vicinity of titanium implants, regardless of the position of the implant. - There were more artifacts in the buccal and lingual region of any implant location and less artifacts in the mesial and distal molars, premolars and canines. - The mesio-buccal, mesio-lingual, disto-buccal, and disto-lingual incisors had less artifacts. - An increase in distance caused a significant decrease in the intensity of the artifact.
Schulze, Berndt, d'Hoedt (2010)[26]	Germany	Experimental - in vitro	- Phantom consisting of a dental stone plaster - For hard and soft tissue simulation, an acrylic water tank was used (diameter: 95 mm, height: 40 mm).	- 3D Accuitomo® - Next Generation i-CAT®	- Accuitomo: 80 kV and 90 kV 4 mA; FOV 6 cm; voxel size 0.125 mm - i-CAT: 120 kV; 4 mA; FOV 6 cm; voxel size 0.250 mm	- ImageJ software (version 133u) - Reconstruction: axial - ROIs: 1: adjacent to the first implant image; 2: adjacent to the second implant image; 3: central area between implants; 4: anterior region to ROI 3 - GV: determined by pixel size: Accuitomo (20 × 20); i-CAT (10 × 10)	- Simulated dental implants: titanium cylinders (4 mm diameter and approximately 12 mm length), TICO, Titan Concept, Berlin, Germany - Implant region: premolar and molar region in the mandible The distance between implants was 22 mm.	Beam-hardening	- In ROI 1 + 2: The Accuitomo (80 kV) had more artifacts than Accuitomo (90 kV) and i-CAT (120 kV). - In ROI 3 and 4: The Accuitomo (90 kV) had more artifacts than Accuitomo (80 kV) and i-CAT (120 kV).	- There were more artifacts in ROI 1 + 2, followed by ROI 3 and ROI 4. This result was independent of the CBCT protocol used, Accuitomo (80 kV and 90 kV) or i-CAT (120 kV).

FOV: field of view, MAR: metal artifact reduction, AR: analysis region, GV: gray value, ROI: region of interest, SD: standard deviation
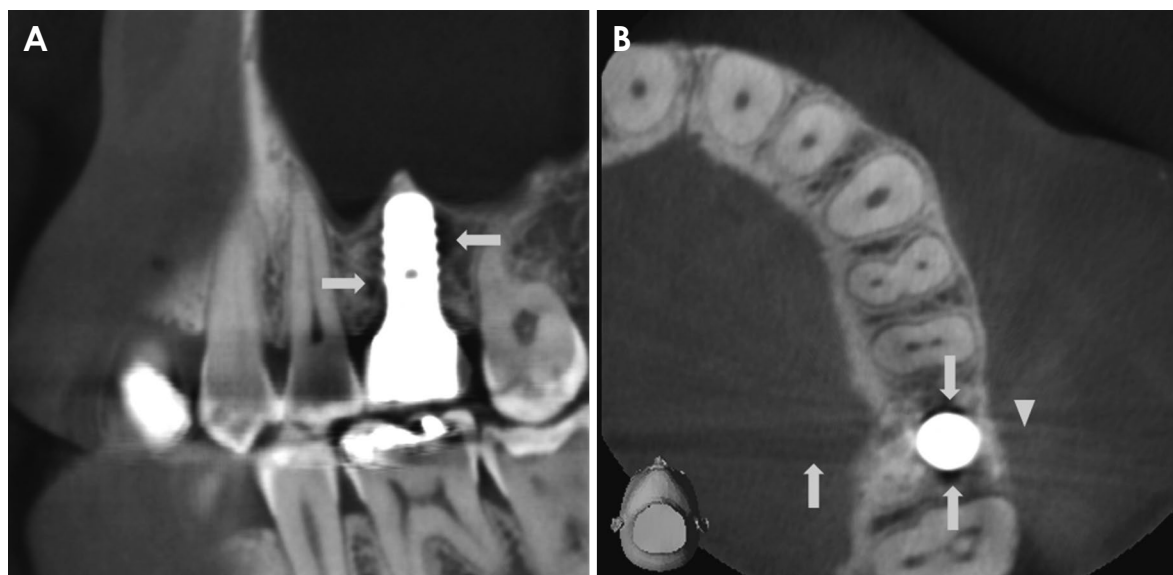
Fig. 2. Parasagittal reconstruction (A) and axial reconstruction (B) cone-beam computed tomographic images show artifacts around a titanium dental implant. The arrows show artifacts (streaking artifacts) and the arrowhead shows a beam-hardening artifact. Tomography model: Accuitomo. Acquisition protocol: voxel size: 0.125 mm; field of view: 6 cm; 90 kV; 7 mA; 30.8 s.

implants. In 2 studies, 5 titanium cylinders were used as an implant simulator.[18,26] Soft tissue was simulated in 3 studies, using gel, water, and wax.[19-21]

Gray values

The gray values show the degree of attenuation of X-rays and represent the density of the tissue.[27] A numerical value of gray, according to the attenuation of the structures, is expressed in each voxel. These values vary due to the characteristics of the technique, such as energy principles, the presence of artifacts, and geometric shape.[28-30] Gray values were calculated in different ways in the studies selected in this review.

Naitoh et al.[24] used the average of the pixel values. In the studies by Martins et al.,[18] Fontenele et al.,[21] Machado et al.,[22] and Schulze et al.,[26] the standard deviations (SDs) of the mean gray values were obtained to express the expression of artifacts. A higher SD of the mean gray value indicated a greater amount of artifacts and worse image quality.

Shokri et al.[20] obtained tomographic images before and after implant insertion. The mean gray values were obtained by analyzing the images with and without implants, and by subtracting these values, the expression of artifacts was obtained.

The average difference in gray values between test and control models as a percentage in each volume of interest was calculated by Benic et al.[25] and Sancho-Puchades et al.[23] Positive values represented the largest formation of artifacts, while negative values represented the least formation.

Types of artifacts

Most studies evaluated the presence of beam-hardening artifacts,[18-23,25,26] and Demirturk Kocasara et al.[19] also evaluated the presence of streaking artifacts. A clinical study evaluated the presence of band-like radiolucent areas around dental implants (Fig. 2).[24]

Presence of artifacts in clinical studies

The clinical studies evaluated beam-hardening artifacts and band-like radiolucent areas around implants, calculated using gray values and the values of pixels, respectively.[22,24]

In the retrospective study, the amount of artifacts in the maxilla and mandible, anterior and posterior region, and isolated and adjacent implants was evaluated.[22] The highest median gray value represented the greatest amount of artifacts. In the mandible, more artifacts were observed in the apical (17.69) and middle (18.48) regions than in the maxilla ($P=0.0024$; $P<0.0001$, respectively). In the anterior region of the jaws, the apical (17.48) and middle (17.93) regions had more artifacts than the posterior region ($P=0.0105$; $P=0.0316$, respectively). No significant difference was found between isolated and adjacent implants in any of the 3 regions evaluated (apical: $P=0.8880$; middle: $P=0.3981$; cervical: $P=0.7553$).

In the prospective study, the highest mean pixel value

was observed in the region between dental implants ($P <$ 0.0001), followed by the region posterior to dental implants ($P < 0.0001$), between dental implants and neighboring teeth ($P = 0.0016$), and between neighboring teeth.[24]

Presence of artifacts in *in vitro* studies

Influence of dental implant materials on the production of artifacts

A total of 306 implants were used in the studies, including titanium (Ti), zirconia (Zr), and titanium-zirconia (TiZr) implants. The Zr implants showed more artifacts than the Ti and TiZr implants.

The Zr implants (3.5-4.5 mm × 10 mm) had higher mean gray values (range: −156% to 269%), than the TiZr (3.3 mm × 10 mm; range: −55% to 87%), Ti (4.1 mm × 10 mm; range: −46% to 98%), and Ti (3.3 mm × 10 mm; range: −11% to 84%) ($P = 0.0167$) implants, corresponding to the greatest amount of artifacts.[23] At different voxel sizes (0.2, 0.25, 0.3 and 0.4 mm), the highest mean gray values were found in Zr implants (229.5, 173.0, 153.5, and 101.5, respectively), followed by Ti grade 4 (62.0, 60.5, 34.5, and 29.0, respectively), Ti grade 5 (34.0, 32.0, 21.0, and 30.0, respectively) and TiZr (54.1, 45.5, 29.5, and 28.5, respectively).[19] When evaluated using different CT scanners (Picasso Trio®; Vatech, Hwaseong, Korea, Pro-Max3D®; Planmeca Oy, Helsinki, Finland, and 3D Accuitomo 80®; Morita, Kyoto, Japan), the mean gray values for Zr implants (61.81, 80.86, and 117.88, respectively) showed a greater amount of artifacts than for Ti implants (56.90, 58.80, and 110.66, respectively) and the control group (55.63, 56.39, and 105.29, respectively).[21]

Influence of bone type on the production of artifacts

Two studies evaluated the formation of artifacts in different types of bones. The first study removed bone cylinders containing cortical and spongy bone from a fresh bovine rib,[18] and the second study collected a cortical bone block from a fresh bovine femur and 2 blocks from a fresh bovine rib, one containing only spongy bone and the other with cortical/spongy bone.[20]

Martins et al.[18] inserted a bone cylinder in the left lower first premolar region (analysis region) in a phantom model, and titanium cylinders were then gradually inserted into holes in the model, starting on the opposite side of where the bone was in the arch, followed by the adjacent side, according to established protocols. The average gray value in the 8 regions of interest (ROIs), around the cortical and spongy bone, were calculated. When analyzing the formation of artifacts in different bone types, it was observed that cortical bone presented a greater amount of artifacts in general compared to cancellous bone ($P < 0.0001$).

In the study conducted by Shokri et al.,[20] Ti implants were inserted into the center of the bone blocks, with wax around them to simulate soft tissue. The spongy bone block (mean gray value: 468.58) showed significantly more artifacts than the block with cortical/spongy bone (mean gray value: 322.63; $P = 0.035$) and the block with only cortical bone (mean gray value: 277.47; $P = 0.007$).

Influence of regions close to the implant with a greater amount of artifacts

The regions close to the implant that presented the greatest amount of artifacts were buccal, mesio-buccal, lingual, and disto-lingual in the region of the lower right premolars,[23] as well as buccal and lingual in the incisor, canine, premolar, and molar regions.[25] In general, all buccal and lingual regions of the implants showed a greater amount of artifacts. In implants in the regions of the second molars, first molars, premolars, and canines, the mesial regions (mean SD: second molars, −50±8; first molars, −55±8; premolars, −32±4; and canines, −9±7) and distal regions (mean SD: second molars, −46±14; first molars, −48±13; premolars, −40±10; and canines, −17±15) were those with the highest negative gray values. In the region of the incisors, the regions with the lowest formation of artifacts were mesio-buccal (mean SD: −6±11), mesio-lingual (mean SD: −15±7), disto-buccal (mean SD: −6±11) and disto-lingual (mean SD: −21±6).[25]

In another study, 2 implants were installed. Adjacent regions (mesial to one implant and distal to another) (Accuitomo® 80 kV: 637.97; Accuitomo® 90 kV: 665; 3DExam® [KaVo Dental GmbH, Biberach, Germany] 120 kV: 973.09) presented a greater amount of artifacts, followed by the region between the implants (Accuitomo® 80 kV: 924.51; Accuitomo® 90 kV: 877.99; 3DExam® 120 kV: 1454.07) and the buccal region between implants (Accuitomo® 80 kV: 1303.50; Accuitomo® 90 kV: 1222.09; 3DExam® 120 kV: 2153.44).[26] One study evaluated the lingual region of the implant at different angles; regions ranging from 65°, 90°, 115° and 140° around the implant presented higher mean gray values in the range of 65° to 115°.[21]

Influence of distance on artifact formation

The relationship between the distance from the generating object and artifact expression was evaluated in 4 studies, all of which found that artifact intensity decreased as the distance from the implant surface increased.[18,21,23,25]

The ROIs in the studies by Benic et al.[25] and Sancho-Puchades et al.[23] were the same, but the implants were placed in different locations. The first study evaluated gray values at 3 distances, and found more artifacts at a distance of 0.5 mm (mean gray value: 45 ± 10), followed by 1 mm (mean gray value: 28 ± 14) and 2 mm (mean gray value: 14 ± 7) from the implant surface. Sancho-Puchades et al.[23] placed the implants only in the edentulous region of tooth 45 and observed a greater amount of artifacts at a distance of 0.5 mm, followed by 1 mm and 2 mm. Fontenele et al.[21] evaluated 11 ROIs. In general, ROIs closer to the implant had greater amounts of artifacts, which managed to reach up to 3.5 cm from the generating object. In the study by Martins et al.,[18] it was possible to observe through the gray value averages that in the presence of the implant cylinder, there were more artifacts when they were in proximity to the analyzed region (protocol E; mean gray value: 53 for OP300 Maxio® [Instrumentarium Dental, Tuusula, Finland] and 71 for Picasso Trio®) (protocol F; mean gray value: 136 for OP300 Maxio® and 200 for Picasso Trio®) than on the opposite and posterior side of the analyzed region (protocol A; mean gray value: 37 for OP300 Maxio® and 45 for Picasso Trio®).

Influence of tomography on the formation of the artifact

Two studies compared 3D Accuitomo (J Morita®) with other CBCT devices. Schulze et al.[26] used different kV values in the protocols for image acquisition. In the Accuitomo® scanner, the values were 80 kV and 90 kV, and in the i-CAT® (Imaging Sciences International, Hatfield, PA, USA), it was 120 kV. In the analysis of the images, it was observed that the kV value influenced the formation of artifacts. The images obtained in the Accuitomo® with 80 kV showed more artifacts in adjacent regions (mesial to one implant and distal to another) than the images obtained using the 90 kV and i-CAT® protocols. Among the implants and buccal to this region, the 90 kV images expressed more artifacts than those obtained using other protocols. The acquisition protocols used by Fontenele et al.[21] differ between the 3 CBCT machines in FOV, scan time, and frame. Accuitomo® showed a greater amount of artifacts (mean gray value: 111.28) than ProMax 3D- Planmeca® (mean gray value: 65.35) or Picasso Trio® (mean gray value: 58.11).

Martins et al.[18] used 2 CBCT machines, including Picasso Trio® and OP300 Maxio®, and their protocols differed only in the size of the FOV (8.5×12 cm and 8×15 cm, respectively); however, the Picasso Trio® showed a greater amount of artifacts (mean gray value: 72.57) in their images, regardless of the implant region protocol, than the OP300 Maxio® (mean gray value: 55.57) ($P < 0.0001$).

Influence of FOV and mA on the production of artifacts

The FOV was found to influence the average gray value, which was used to assess the production of artifacts. When analyzing larger (6×8 cm^2) and smaller (4×6 cm^2) FOVs, it was found that the size of the FOV was directly proportional to the amount of artifacts; therefore, a larger FOV produced a greater amount of artifacts. In contrast, the mA setting (4 mA vs. 10 mA) did not influence the amount of artifacts around dental implants.[20]

Influence of voxel size on the production of artifacts

Demirturk Kocasara et al.[19] used 4 different voxel sizes to acquire CBCT images: 0.2 mm, 0.25 mm, 0.3 mm, and 0.4 mm. The images with smaller voxel sizes showed a greater amount of artifacts, with the 0.2-mm voxels (mean gray value: 94.9) having the most artifact formation, followed by the 0.25-mm voxels (mean gray value: 77.75). The 0.3-mm voxels (mean gray value: 59.63) and 0.4-mm voxels (mean gray value: 47.25) presented a smaller and similar amount of artifacts.

Discussion

The production of artifacts in CBCT images is a detrimental factor for the interpretation of the examination and diagnosis. It is necessary to be familiar with the various types of artifacts and their causes to minimize them.

An image artifact is a structure that is not present in the tomography object, but is visualized next to the image formed by the data used in the reconstruction. Its origin may be due to physical factors of the device or related to image acquisition.[9,26]

The beam-hardening effect can be explained by the fact that high-density X-rays are partially absorbed by implants. Because they are made of very dense materials, only the most intense X-rays penetrate dental implants, generating artifacts related to beam hardening. The result is the presence of shiny bands, as the implant area in the final image has greater intensity than the other structures. In the region between 2 implants, there may be another type of artifact related to beam hardening, which causes dark bands between the implants.[8,26]

In dentistry, materials such as amalgam (Hg, with an atomic number [Z] of 80; Ag, Z $= 47$) produce artifacts on CBCT.[23,26] The production of artifacts is related to the

atomic number and the density of the materials, and the enamel structures ($Z = 15.6$; $r = 2.94$ g/cm^3), dentin ($Z = 13.7$; $r = 2.42$ g/cm^3) and cortical bone ($Z = 13.2$; $r = 1.9$ g/cm^3), have an atomic number and density lower than that of Ti ($Z = 22$).[31,32] The beam-hardening artifact is the most commonly reported artifact in implantology. Since a metallic object inside the FOV has a similar action to a filter, artifacts are generated in proportion to the atomic number of the metal.[26] In the studies in this review, Zr (ZrO$_2$) implants showed a greater amount of artifacts than Ti and TiZr implants. The production of artifacts is related to the radiopacity of the material used, which is also directly related to its atomic number (Z). Therefore, the difference in the amount of artifacts in CBCT between Ti, TiZr, and Zr implants reflects the differences in the atomic numbers of Ti ($Z = 22$), Zr ($Z = 40$), and O$_2$ ($Z = 8$).[19,21,23] The greater the atomic number, the greater the radiopacity and consequently, the greater production of artifacts; these relationships explain the difference in the amount of artifacts between the different types of dental implant materials.

A higher FOV and a lower kVp resulted in greater production of beam-hardening artifacts in CBCTs in the presence of dental implants. Other factors, such as the thickness of the tissue in the maxilla and mandible and the geometry of the cone-shaped X-ray beam in different anatomical sites, can alter the pattern of scattered radiation and affect the production of beam hardening.[33] Higher kVp values can reduce the production of artifacts due to the difference between low- and high-energy beams in attenuation by high-density objects;[26] however, the devices that allow this change have a range of 60 to 90 kVp, while in CBCT, the kVp values are mostly between 80 and 120 kVp.[34]

Some factors can influence gray value variability, which may explain differences in results between similar studies. Gray values can vary within the same image if the region evaluated within the FOV is more central or peripheral.[30,35] Fontenele et al.[21] evaluated gray values in ROIs in 4 angulations in the lingual region of the arch, perhaps the area with the greatest amount of artifacts, did not coincide with the ROI. Even with this methodology, artifacts were still present at a distance of 3.5 cm.

Other factors that can influence gray values are endomass and the presence of exo-mass. Defined as structures that are beyond the FOV limit,[36] a smaller FOV has more exo-mass.[29] According to the study by Oliveira et al.[29] which used a thin layer of water as an exo-mass, the gray value variability was reduced in its presence. The use of water and air as an endo-mass showed a larger variation in gray values in the presence of air than in the presence of water.[37] These factors could explain the differences between the results of studies that simulated the presence of soft tissue and those that did not.

Gray values can also vary depending on the material of the phantom. According to Oliveira et al.,[29] a higher the concentration of the material leads to a greater the predisposition to the beam-hardening effect, thereby reducing the image quality.

The clinical study by Machado et al.[22] measured the amount of artifacts according to the difference between the maximum and minimum gray values of the same CBCT scan, and they did not find a statistically significant difference between the amount of artifacts in the regions of isolated and adjacent implants. These findings can be explained by the size of the ROI evaluated (10×10 mm), which exerted little or no effects on neighboring implants. Their study reported a greater amount of artifacts in the cervical third of the dental implant, probably due to the presence of the prosthesis on the implant, since the atomic numbers of prosthetic alloy materials, such as cobalt-chromium, are higher than that of Ti. More severe artifacts were also observed in the mandibular and anterior region (incisors and canines), and it was found that the variety in gray values was affected by the location and adjacent anatomical structures, consistent with Oliveira et al.[33] who demonstrated that the same object could present varying gray values according to the anatomical location. Valizadeh et al.[38] found that the location of the object in the FOV affects the gray values through the interactions of X-rays and adjacent structures. The effect of the exo-mass (i.e., the entire craniofacial area outside the FOV) can also explain the variation of artifacts according to the anatomical area. Thus, structures such as the skull and spine affect the measurements of gray values in the maxilla and mandible.[23,39]

Artifacts are evaluated using pixel values; thus, the greatest amount of artifacts was found in the region between dental implants in CBCT images, probably due to the higher density in the presence of metallic implants.[24] A lack of specificity of the ROI was observed in terms of its size and location, as well as the level of evaluation in axial images. The values of Hounsfield units are absolute,[40-42] and cannot be used to evaluate metal artifacts, because pixel values are not absolute in CBCT.[43]

The artifacts caused by the presence of implants change the visibility of the bone, making them difficult to assess.[44] The studies in this review evaluated the formation of artifacts in cortical and spongy bone. Despite having the same basic histological structure, cortical bone differs in being more compact and mineralized, while spongy bone has in-

tercommunicating cavities that decrease its density.[45] Martins et al.[18] observed a greater amount of artifacts in cortical bone, while Shokri et al.[20] observed this result for cancellous bone. The presence of a greater amount of artifacts in cortical bone is explained by its high mineral density, which makes the effect of beam-hardening artifacts more pronounced.[18,46] However, Shokri et al.[20] considered that greater bone density around the implant has the same effect as an increase in kVp, following the results of Schulze et al.,[26] since low-energy photons are absorbed by high-density bone and fewer photons, with greater energy, reach the implant. Thus, the amount of artifacts in denser bone is lower, while in trabecular bone, with less density, it is greater. The first study used a polymethyl methacrylate phantom and placed a bone cylinder in the anterior region and implants in other positions of the arch to evaluate artifacts, while the second used a bone block with an implant inside and a surrounding wax model, simulating soft tissues. These differences in methodology may be responsible for the divergent results, since wax better simulates clinical conditions, with appropriate heterogeneity, and affects the gray value measurements in the evaluated region, whereas polymethyl methacrylate is homogeneous.

In general, the buccal and lingual regions of the implant showed a greater amount of artifacts,[23,25] as well as the adjacent regions, mesial to one implant and distal to another.[26] Sancho-Puchades et al.[23] and Benic et al.[25] used the same parameters for ROI in the mandible. Fontenele et al.[21] used different angulations in the lingual region outside the bone area from the implant in the mandible. Schulze et al.[26] used the parameter from the insertion of 2 implants in the mandible, which caused a disparity between their results and those of the other studies. The intensity of the artifacts decreased as the implant distance increased, corroborating other studies.[18,21,23,25] The artifacts can reach a distance of up to 3.5 cm from the implant, depending on the CBCT device.[21]

According to Pauwels et al.,[30] it would be ideal to use more than 1 tomography model in research, because the technical differences between devices mean that the conclusions of a study using a certain model may not be applied to other CBCT devices without an experimental check. Three of the studies included in this review used more than 1 tomography model in their experiments.[18,21,26]

In the 2 studies that evaluated Accuitomo®, it presented more artifacts than the other CT scanners (i-CAT®, Picasso Trio®, and ProMax 3D®).[21,26] Martins et al.[18] showed that the OP300 Maxio® had fewer artifacts than the Picasso Trio®. Through these data, we can conclude that when considering grayscale measurements, the CT scanner that presented the fewest artifacts in the presence of implants would be the OP300 Maxio®, followed by ProMax 3D®, Picasso Trio®, and Accuitomo®. The i-CAT® (120 kVp) showed fewer artifacts than the Accuitomo® (80 and 90 kVp).

Higher-resolution images show greater artifact formation than lower-resolution images due to the smaller voxel size because fewer X-ray photons are detected. Using larger voxels enables higher image quality and fewer artifacts, and therefore less radiation exposure.[19] However, the size of the FOV must be considered, since it influences the radiation dose of the exam. Paulwels et al.[34] reported no improvement in the amount of artifacts in high-dose protocols, although some devices showed improvement with a high exposure and large FOV, unlike Shokri et al.,[20] who reported that a larger FOV resulted in an increase in artifacts; however, changes in mA did not influence the amount of metal artifacts.

The beam-hardening artifact is the most commonly reported artifact around dental implants in CBCT exams. Some factors such as the implant material (Zr), larger FOVs, tomography model (Accuitomo®), lower kV, and smaller voxels favor the formation of these artifacts. Although inevitable, there are fewer artifacts with titanium implants and the artifacts can be minimized in protocols with smaller FOVs, larger voxels, and higher kV, which favor the reduction of artifacts generated by dental implants, and, consequently, improve image quality. The presence of artifacts can lead to misdiagnoses, so the clinical examination and complementary radiographs are essential for proper diagnoses in implantology.

Conflicts of Interest: None

References

1. Scarfe WC, Farman AG, Sukovic P. Clinical applications of cone-beam computed tomography in dental practice. J Can Dent Assoc 2006; 72: 75-80.
2. Scarfe WC, Farman AG. What is cone-beam CT and how does it work? Dent Clin North Am 2008; 52: 707-30.
3. White SC. Cone-beam imaging in dentistry. Health Phys 2008; 95: 628-37.
4. Scarfe WC, Li Z, Aboelmaaty W, Scott SA, Farman AG. Maxillofacial cone beam computed tomography: essence, elements and steps to interpretation. Aust Dent J 2012; 57(Suppl 1): 46-60.
5. Ruprecht A. Oral and maxillofacial radiology: then and now. J Am Dent Assoc 2008; 139(Suppl): 5S-6S.
6. Nagarajappa AK, Dwivedi N, Tiwari R. Artifacts: the downturn of CBCT image. J Int Soc Prev Community Dent 2015; 5: 440-5.
7. Loubele M, Maes F, Jacobs R, Van Steenberghe D, White SC,

Suetens P. Comparative study of image quality for MSCT and CBCT scanners for dentomaxillofacial radiology applications. Radiat Prot Dosimetry 2008; 129: 222-6.

8. Schulze R, Heil U, Gross D, Bruellmann DD, Dranischnikow E, Schwanecke U, et al. Artifacts in CBCT: a review. Dentomaxillofac Radiol 2011; 40: 265-73.

9. Draenert FG, Coppenrath E, Herzog P, Müller S, Mueller-Lisse UG. Beam hardening artefacts occur in dental implant scans with the NewTom cone beam CT but not with the dental 4-row multidetector CT. Dentomaxillofac Radiol 2007; 36: 198-203.

10. Nardi C, Molteni R, Lorini C, Taliani GG, Matteuzzi B, Mazzoni E, et al. Motion artefacts in cone beam CT: an in vitro study about the effects on the images. Br J Radiol 2016; 89: 20150687.

11. Zhu L, Chen Y, Yang J, Tao X, Xi Y. Evaluation of the dental spectral cone beam CT for metal artefact reduction. Dentomaxillofac Radiol 2019; 48: 20180044.

12. Vasconcelos TV, Nascimento EH, Bechara BB, Freitas DQ, Noujeim M. Influence of cone beam computed tomography settings on implant artifact production: zirconia and titanium. Int J Oral and Maxillofac Implants 2019; 34: 1114-20.

13. Alawaji Y, MacDonald DS, Giannelis G, Ford NL. Optimization of cone beam computed tomography image quality in implant dentistry. Clin Exp Dent Res 2018; 4: 268-78.

14. Kerkfeld V, Meyer U. Higher resolution in cone beam computed tomography is accompanied by improved bone detection in peri-implant bone despite metal artifact presence. Int J Oral Maxillofac Implants 2018; 33: 1331-8.

15. Gao L, Sun H, Lin T, Sui J, Ni X. Metal artifact reduction for dental implants in kilovoltage computed tomography using megavoltage cone-beam computer tomography. Sheng Wu Yi Xue Gong Cheng Xue Za Zhi 2017; 34: 730-7.

16. de-Azevedo-Vaz SL, Peyneau PD, Ramirez-Sotelo LR, Vasconcelos Kde F, Campos PS, Haiter-Neto F. Efficacy of a cone beam computed tomography metal artifact reduction algorithm for the detection of peri-implant fenestrations and dehiscences. Oral Surg Oral Med Oral Pathol Oral Radiol 2016; 121: 550-6.

17. Carrafiello G, Dizonno M, Colli V, Strocchi S, Pozzi Taubert S, Leonardi A, et al. Comparative study of jaws with multislice computed tomography and cone-beam computed tomography. Radiol Med 2010; 115: 600-11.

18. Martins LAC, Queiroz PM, Nejaim Y, Vasconcelos KF, Groppo FC, Haiter-Neto F. Evaluation of metal artefacts for two CBCT devices with a new dental arch phantom. Dentomaxillofac Radiol 2020; 49: 20190385.

19. Demirturk Kocasarac H, Ustaoglu G, Bayrak S, Katkar R, Geha H, Deahl ST 2nd, et al. Evaluation of artifacts generated by titanium, zirconium, and titanium-zirconium alloy dental implants on MRI, CT, and CBCT images: a phantom study. Oral Surg Oral Med Oral Pathol Oral Radiol 2019; 127: 535-44.

20. Shokri A, Jamalpour MR, Khavid A, Mohseni Z, Sadeghi M. Effect of exposure parameters of cone beam computed tomography on metal artifact reduction around the dental implants in various bone densities. BMC Med Imaging 2019; 19: 34.

21. Fontenele RC, Nascimento EH, Vasconcelos TV, Noujeim M, Freitas DQ. Magnitude of cone beam CT image artifacts related to zirconium and titanium implants: impact on image quality. Dentomaxillofac Radiol 2018; 47: 20180021.

22. Machado AH, Fardim KAC, de Souza CF, Sotto-Maior BS, Assis NMSP, Devito KL. Effect of anatomical region on the formation of metal artefacts produced by dental implants in cone beam computed tomographic images. Dentomaxillofac Radiol 2018; 47: 20170281.

23. Sancho-Puchades M, Hämmerle CH, Benic GI. In vitro assessment of artifacts induced by titanium, titanium-zirconium and zirconium dioxide implants in cone-beam computed tomography. Clin Oral Implants Res 2015; 26: 1222-8.

24. Naitoh M, Saburi K, Gotoh K, Kurita K, Ariji E. Metal artifacts from posterior mandibular implants as seen in CBCT. Implant Dent 2013; 22: 151-4.

25. Benic GI, Sancho-Puchades M, Jung RE, Deyhle H, Hämmerle CH. In vitro assessment of artifacts induced by titanium dental implants in cone beam computed tomography. Clin Oral Implants Res 2013; 24: 378-83.

26. Schulze RK, Berndt D, d'Hoedt B. On cone-beam computed tomography artifacts induced by titanium implants. Clin Oral Implants Res. 2010; 21: 100-7.

27. Valiyaparambil JV, Yamany I, Ortiz D, Shafer DM, Pendrys D, Freilich M, et al. Bone quality evaluation: comparison of cone beam computed tomography and subjective surgical assessment. Int J Oral Maxillofac Implants 2012; 27: 1271-7.

28. Parsa A, Ibrahim N, Hassan B, Motroni A, van der Stelt P, Wismeijer D. Reliability of voxel gray values in cone beam computed tomography for preoperative implant planning assessment. Int J Oral Maxillofac Implants 2012; 27: 1438-42.

29. Oliveira ML, Freitas DQ, Ambrosano GM, Haiter-Neto F. Influence of exposure factors on the variability of CBCT voxel values: a phantom study. Dentomaxillofac Radiol 2014; 43: 20140128.

30. Pauwels R, Jacobs R, Singer SR, Mupparapu M. CBCT-based bone quality assessment: are Hounsfield units applicable? Dentomaxillofac Radiol 2015; 44: 20140238.

31. Suzuki Y, Shimano T. The effective atomic number of the teeth. Shika Hoshasen 1976; 16: 63-72.

32. Hiraoka T, Kawashima K, Hoshino K, Takayama T, Narai K. Development of bone substitute materials. CODEN HCSKE 1987; suppl.4: 93-6.

33. Oliveira ML, Tosoni GM, Lindsey DH, Mendoza K, Tetradis S, Mallya SM. Influence of anatomical location on CT numbers in cone beam computed tomography. Oral Surg Oral Med Oral Pathol Oral Radiol 2013; 115: 558-64.

34. Pauwels R, Stamatakis H, Bosmans H, Bogaerts R, Jacobs R, Horner K, et al. Quantification of metal artifacts on cone beam computed tomography images. Clin Oral Implants Res 2013; 24: 94-9.

35. Katsumata A, Hirukawa A, Okumura S, Naitoh M, Fujishita M, Ariji E, et al. Effects of image artifacts on gray-value density in limited-volume cone-beam computerized tomography. Oral Surg Oral Med Oral Pathol Oral Radiol Endod 2007; 104: 829-36.

36. Bryant JA, Drage NA, Richmond S. Study of the scan uniformity from an i-CAT cone beam computed tomography dental imaging system. Dentomaxillofac Radiol 2008; 37: 365-74.

37. Nomura Y, Watanabe H, Shirotsu K, Honda E, Sumi Y, Kura-

bayshi T. Stability of voxel values from cone-beam computed tomography for dental use in evaluating bone mineral content. Clin Oral Implants Res 2013; 24: 543-8.

38. Valizadeh S, Vasegh Z, Rezapanah S, Safi Y, Khaeazifard MJ. Effect of object position in cone beam computed tomography field of view for detection of root fractures in teeth with intra-canal posts. Iran J Radiol 2015; 12: e25272.

39. Smeets R, Schöllchen M, Gauer T, Aarabi G, Assaf AT, Ren-denbach C, et al. Artefacts in multimodal imaging of titanium, zirconium and binary titanium-zirconium alloy dental implants: an in vitro study. Dentomaxillofac Radiol 2017; 46: 20160267.

40. Resnik RR, Kircos LT, Misch CE. Diagnostic imaging and techniques. In: Misch CE, Contemporary Implant Dentistry. 3rd ed. St. Louis, MO: Mosby; 2008. p. 38-67.

41. Naitoh M, Kurosu Y, Inagaki K, Katsumata A, Noguchi T, Ariji E. Assessment of mandibular buccal and lingual cortical bones in postmenopausal women. Oral Surg Oral Med Oral Pathol Oral Radiol Endod 2007; 104: 545-50.

42. Norton MR, Gamble C. Bone classification: an objective scale of bone density using the computerized tomography scan. Clin Oral Implants Res 2001; 12: 79-84.

43. Naitoh M, Katsumata A, Mitsuya S, Kamemoto H, Ariji E. Measurement of mandibles with microfocus x-ray computer-ized tomography and compact computerized tomography for dental use. Int J Oral Maxillofac Implants 2004; 19: 239-46.

44. Razavi T, Palmer RM, Davies J, Wilson R, Palmer PJ. Accura-cy of measuring the cortical bone thickness adjacent to dental implants using cone beam computed tomography. Clin Oral Implants Res 2010; 21: 718-25.

45. Junqueira LC, Carneiro J. Histologia básica. 10th ed. Rio de Janeiro: Guanabara Koogan S.A.; 2004.

46. Arisan V, Karabuda ZC, Avsever H, Özdemir T. Convencional multi-slice computed tomography (CT) and cone-beam CT (CBCT) for computer-assisted implant placement. Part I: rela-tionship of radiographic gray density and implant stability. Clin Implant Dent Relat Res 2013; 15: 893-906.